Pion-nucleon scattering to order p^4 in SU(3) heavy baryon chiral perturbation theory

Bo-Lin Huang [*]

Department of Physics, Jishou University, Jishou 416000, China

We calculate the T matrices of elastic pion-nucleon (πN) scattering up to fourth order in SU(3) heavy baryon chiral perturbation theory. The pertinent low-energy constants are determined by fitting to πN phase shifts below the 200 MeV pion laboratory momentum in the physical region. The scattering lengths and scattering volumes are extracted from the chiral amplitudes, and turn out to be in good agreement with those of other approaches and the available experimental values. We also discuss the subthreshold parameters and the related issues. On the basis of the various phase shifts, the threshold parameters and the subthreshold parameters, the convergence of the chiral expansion is analyzed in detail. The calculation provides the possibility to consider explicitly more complex processes involving strangeness.

I. INTRODUCTION

Chiral perturbation theory (ChPT) allows one to analyze hadronic processes at low energies that are not accessible by a perturbative expansion in the strong coupling constant α_s of quantum chromodynamics (QCD) [1–4]. ChPT is an efficient framework to calculate in a model-independent way, e.g., the amplitudes of pion-nucleon (πN) scattering below the chiral symmetry breaking scale $\Lambda_\chi \simeq 1$ GeV. However, there exists a power-counting problem in baryon ChPT because of the nonvanishing baryon mass M_0 in the chiral limit. Over the years, several approaches have been proposed to solve this problem. Heavy baryon ChPT (HBχPT) [5,6], the infrared regularization of covariant baryon ChPT [7], and the extended-on-mass-shell scheme for baryon ChPT [8,9] are some popular approaches. The last two approaches are fully relativistic and have lead to substantial progress in many aspects as documented in Refs. [10–16]. However, the expressions from the loop diagrams become rather complicated in these fully relativistic approaches [17–19]. On the other hand, HBχPT is a well-established and versatile tool for the study of low-energy hadronic processes. The amplitudes in HBχPT proceeds simultaneously in terms of p/Λ_χ (nonrelativistic contributions from tree and loop diagrams) and p/M_0 (relativistic corrections), where p denotes the meson momentum (or mass) or the small residual momentum of a baryon in a low-energy process.

In recent years, there has been renewed interest in theoretical studies of elastic meson-baryon scattering at low energies. These are not only concerned with the description of the strong mesonic interaction, but also with the chiral properties of the baryons. The low-energy processes between pions and nucleons have been investigated extensively in SU(2) HBχPT in Refs. [20–23]. Furthermore, the subthreshold parameters of pion-nucleon scattering have also been deeply studied by combining the Roy-Steiner (RS) equations and SU(2) ChPT [24,25]. For processes involving kaons or hyperons, the situation becomes more involved, since one has to work out the consequences of three-flavor chiral dynamics. In a previous paper [26] we have investigated KN and $\bar{K}N$ elastic scattering up to one-loop order in SU(3) HBχPT by fitting low-energy constants to partial-wave phase shifts of KN scattering and obtained quite reasonable results. This approach was then extended by predicting the amplitudes of pseudoscalar-meson octet-baryon scattering in all channels, with the pertinent low-energy constants fitted to partial-wave phase shifts of elastic πN and KN scattering [27]. At this point one should note that the detailed predictions of SU(3) HBχPT for the meson-baryon scattering lengths have been given previously in Refs. [28–32]. Moreover, these studies in SU(3) HBχPT has been extended to partial-wave phase shifts, the pion-nucleon sigma term, and other quantities. In a recent paper [33], we have calculated the complete T matrices of pion-nucleon scattering up to third order in SU(3) HBχPT and obtained as a byproduct nucleon properties, like the pion-nucleon sigma term $\sigma_{\pi N}$. A good description of the phase shifts of πN scattering below 200 MeV has been obtained, and then it can serve as a consistency check to consider also the other meson-baryon scattering channels. However, no good convergence of the chiral expansion is observed in calculations that terminate at third order. Therefore, we will compute in this paper the T matrices for πN scattering up to fourth order in SU(3) HBχPT. The pertinent low-energy

constants (LECs) will be determined by fitting to empirical S- and P-wave phase shifts of πN scattering. In particular, the LECs related to contact terms of chiral dimension will be obtained separately. The threshold parameters, the subthreshold parameters, and the related issues will be discussed briefly. At last, the convergence of the chiral expansions will also be analyzed and discussed in detail.

The present paper is organized as follows. In Sec. II, we summarize the Lagrangians involved in the evaluation of the fourth-order contributions. In Sec. III, we present some explicit expressions for the T matrices of elastic πN scattering at order p^4. In Sec. IV, we outline how to derive phase shifts, scattering lengths, and scattering volumes from the T matrices. Section V contains the presentation and discussion of our results and it also includes a brief summary. Appendixes A and B contain the expressions for the scattering lengths and the subthreshold parameters, respectively.

II. CHIRAL LAGRANGIAN

In order to calculate the pion-nucleon scattering amplitude up to order p^4 in SU(3) heavy baryon chiral perturbation theory, one has to evaluate tree and loop diagrams with vertices from the effective chiral Lagrangian:

$$\mathcal{L}_{\text{eff}} = \mathcal{L}_{\phi\phi}^{(2)} + \mathcal{L}_{\phi B}^{(1)} + \mathcal{L}_{\phi B}^{(2)} + \mathcal{L}_{\phi B}^{(3)} + \mathcal{L}_{\phi B}^{(4)}. \qquad (1)$$

These Lagrangians are written in terms of the traceless Hermitian 3×3 matrices ϕ and B that include the pseudoscalar Goldstone boson fields (π, K, $\bar{K}$, η) and the octet-baryon fields (N, Λ, Σ, Ξ), respectively. The explicit form of the $\mathcal{L}_{\phi\phi}^{(2)}$, $\mathcal{L}_{\phi B}^{(1)}$, $\mathcal{L}_{\phi B}^{(2)}$, and $\mathcal{L}_{\phi B}^{(3)}$ can be found in Ref. [33]. The complete fourth-order heavy baryon Lagrangian $\mathcal{L}_{\phi B}^{(4)}$ naturally splits up into two parts: relativistic corrections with fixed coefficients and counterterms proportional to new low-energy constants. The relativistic terms can be obtained from the original leading order, next-to-leading order, and next-to-next-to-leading order Lorentz-invariant Lagrangians through path integral manipulations [6]. For three-flavors and at chiral order four, the Lorentz-invariant meson-baryon Lagrangian has been constructed in Ref. [34] and we can obtain from it the counterterms

relevant for our purpose. Since the dimension-four chiral meson-baryon Lagrangian $\mathcal{L}_{\phi B}^{(4)}$ is very lengthy, the explicit expressions will not be given in this paper, where we consider only elastic pion-nucleon scattering. Of course, the expansions in SU(3) and SU(2) HBχPT are consistent with each other. For this reason the notation of low-energy constants $\bar{e}_i(i = 14, \ldots, 22, 35, \ldots, 38)$ for the fourth-order counterterms in SU(2) HBχPT introduced in Ref. [21] will also be used in this paper.

III. T MATRICES FOR PION-NUCLEON SCATTERING

We are considering the elastic pion-nucleon scattering process $\pi(q) + N(p) \rightarrow \pi(q') + N(p')$ in the center-of-mass system. In states with total isospin $I = 1/2$ or $I = 3/2$ of the pion-nucleon system, the corresponding T matrix takes the following form in spin space:

$$T_{\pi N}^{(I)} = V_{\pi N}^{(I)}(w, t) + i\boldsymbol{\sigma} \cdot (\boldsymbol{q}' \times \boldsymbol{q})W_{\pi N}^{(I)}(w, t) \qquad (2)$$

where $w = q_0 = q_0' = (m_\pi^2 + \boldsymbol{q}^2)^{1/2}$ is the pion center-of-mass energy, and $t = (q' - q)^2 = 2\boldsymbol{q}^2(z - 1)$ is the invariant momentum transfer squared with $z = \cos\theta$ the cosine of the angle θ between $\boldsymbol{q}$ and $\boldsymbol{q}'$. Based on relativistic kinematics, one gets the relation:

$$\boldsymbol{q}'^2 = \boldsymbol{q}^2 = \frac{M_N^2 \boldsymbol{p}_{\text{lab}}^2}{m_\pi^2 + M_N^2 + 2M_N\sqrt{m_\pi^2 + \boldsymbol{p}_{\text{lab}}^2}}, \qquad (3)$$

where $\boldsymbol{p}_{\text{lab}}$ denotes the momentum of the incident meson in the laboratory system. Furthermore, $V_{\pi N}^{(I)}(w, t)$ refers to the non-spin-flip pion-nucleon scattering amplitude and $W_{\pi N}^{(I)}(w, t)$ is called the spin-flip pion-nucleon scattering amplitude.

From leading order $\mathcal{O}(p)$ up to third order $\mathcal{O}(p^3)$, the expressions for the amplitudes $V_{\pi N}^{(I)}(w, t)$ and $W_{\pi N}^{(I)}(w, t)$ can be found in Ref. [33]. At fourth order $\mathcal{O}(p^4)$, the SU(3) results for the πN amplitudes from tree diagrams are essentially the same as those calculated in SU(2) HBχPT in Ref. [21]. After an appropriate renaming of the low-energy constants, these contributions read

$$V_{\pi N}^{(3/2,\text{N3LO})} = -\frac{(D + F)^2}{32M_0^3 w^4 f_\pi^2}[(t^4 + 7t^3 w^2 + 11t^2 w^4 - 3tw^6 + 4w^8) - (11t^3 + 49t^2 w^2 + 32tw^4 + 4w^6)m_\pi^2$$

$$+ (45t^2 + 110tw^2 + 26w^4)m_\pi^4 - 3(27t + 26w^2)m_\pi^6 + 54m_\pi^8] + \frac{m_\pi^2 - w^2}{32M_0^3 f_\pi^2}(4m_\pi^2 - t - 4w^2)$$

$$+ \frac{1}{16M_0^2 f_\pi^2}[4C_0(t + 2w^2 - 2m_\pi^2)m_\pi^2 + C_1(2t^2 + 4tw^2 - 8tm_\pi^2 - 8w^2 m_\pi^2 + 8m_\pi^4)$$

$$+ 4C_2(3tw^2 + 14w^4 - 4tm_\pi^2 - 22w^2m_\pi^2 + 8m_\pi^4) + 2C_3(-t^2 - 4tw^2 + 4tm_\pi^2)] - \frac{8}{M_0 f_\pi^2} C_0 C_2 w^2 m_\pi^2$$

$$+ \frac{1}{2M_0 f_\pi^2}[H_1(4m_\pi^2 - t - 4w^2)m_\pi^2 + H_2(4w^2 + t - 4m_\pi^2)t + 3H_3(4m_\pi^2 - t - 4w^2)w^2 + 2H_4 w^2 t]$$

$$+ \frac{1}{f_\pi^2}[4\bar{e}_{14}(4m_\pi^4 - 4m_\pi^2 t - t^2) + 8\bar{e}_{15}(2w^2 m_\pi^2 - tw^2) + 16\bar{e}_{16}w^4], \tag{4}$$

$$W_{\pi N}^{(3/2,\text{N3LO})} = \frac{(D+F)^2}{16M_0^3 w^4 f_\pi^2}[(t^3 + 5t^2 w^2 + 3tw^4 - w^6) - (9t^2 + 25tw^2 + 4w^4)m_\pi^2$$

$$+ 3(9t + 10w^2)m_\pi^4 - 27m_\pi^6] + \frac{w^2 - m_\pi^2}{16M_0^3 f_\pi^2} + \frac{1}{8M_0^2 f_\pi^2}[8C_0 m_\pi^2 + C_1(2t - 4m_\pi^2)$$

$$- 4C_2 w^2 - 2C_3(t + 2w^2 - 2m_\pi^2)] + \frac{1}{2M_0 f_\pi^2}H_4(8w^2 + t - 4m_\pi^2)$$

$$+ \frac{1}{f_\pi^2}[\bar{e}_{17}(-8m_\pi^2 + 4t) - 8\bar{e}_{18}w^2], \tag{5}$$

$$V_{\pi N}^{(1/2,\text{N3LO})} = \frac{(D+F)^2}{64M_0^3 w^4 f_\pi^2}[(t^4 + 7t^3 w^2 + 11t^2 w^4 + 16w^8) - (11t^3 + 49t^2 w^2 + 32tw^4$$

$$+ 16w^6)m_\pi^2 + 5(9t^2 + 22tw^2 + 4w^4)m_\pi^4 - 84(t + w^2)m_\pi^6 + 60m_\pi^8]$$

$$+ \frac{w^2 - m_\pi^2}{16M_0^3 f_\pi^2}(4m_\pi^2 - t - 4w^2) + \frac{1}{8M_0^2 f_\pi^2}[2C_0(t + 2w^2 - 2m_\pi^2)m_\pi^2 + C_1(t^2 + 2tw^2$$

$$- 4tm_\pi^2 - 4w^2 m_\pi^2 + 4m_\pi^4) + 2C_2(3tw^2 + 14w^4 - 4tm_\pi^2 - 22w^2 m_\pi^2 + 8m_\pi^4)$$

$$+ 2C_3(t^2 + 4tw^2 - 4tm_\pi^2)] - \frac{8}{M_0 f_\pi^2}C_0 C_2 w^2 m_\pi^2 + \frac{1}{M_0 f_\pi^2}[H_1(-4m_\pi^2 + t + 4w^2)m_\pi^2$$

$$- H_2(4w^2 + t - 4m_\pi^2)t - 3H_3(4m_\pi^2 - t - 4w^2)w^2 + H_4 w^2 t]$$

$$+ \frac{1}{f_\pi^2}[4\bar{e}_{14}(4m_\pi^4 - 4m_\pi^2 t - t^2) + 8\bar{e}_{15}(2w^2 m_\pi^2 - tw^2) + 16\bar{e}_{16}w^4], \tag{6}$$

$$W_{\pi N}^{(1/2,\text{N3LO})} = \frac{(D+F)^2}{32M_0^3 w^4 f_\pi^2}[(-t^3 - 5t^2 w^2 - 3tw^4 + 4w^6) + (9t^2 + 25tw^2 + 4w^4)m_\pi^2$$

$$- 3(9t + 10w^2)m_\pi^4 + 24m_\pi^6] + \frac{m_\pi^2 - w^2}{8M_0^3 f_\pi^2} + \frac{1}{4M_0^2 f_\pi^2}[-2C_0 m_\pi^2 + C_1(t - 2m_\pi^2) - 2C_2 w^2$$

$$+ 2C_3(t + 2w^2 - 2m_\pi^2)] + \frac{H_4}{2M_0 f_\pi^2}(8w^2 + t - 4m_\pi^2) + \frac{8}{f_\pi^2}[\bar{e}_{17}(2m_\pi^2 - t) + 2\bar{e}_{18}w^2], \tag{7}$$

where C_i ($i = 0, 1, 2, 3$) and H_i ($i = 1, 2, 3, 4$) are linear combinations of low-energy constants defined in Eqs. (22) and (27) of Ref. [33], respectively. For the dimension-four LECs, we follow the same strategy as in Ref. [21]. The subset of dimension-four low-energy constants $\bar{e}_i$ ($i = 19$, 20, 21, 22, 35, 36, 37, 38) can be absorbed onto the dimension-two LECs c_i ($i = 1, 2, 3, 4$), see Eq. (3.23) in Ref. [21]. We note that, the dimension-two LECs c_i ($i = 1$, 2, 3, 4) introduced in SU(2) HBχPT can be replaced equivalently by the combinations of LECs C_i ($i = 0, 1, 2$, 3) of SU(3) HBχPT. Thus, $\bar{e}_i$ ($i = 14, 15, 16, 17, 18$) are the five remaining dimension-four LECs that are relevant in

our calculation. At fourth order, additional πN amplitudes from one-loop diagrams must be taken into account. The pertinent one-loop diagrams generated by the interaction vertices from $\mathcal{L}_{\phi\phi}^{(2)}$, $\mathcal{L}_{\phi B}^{(1)}$ and $\mathcal{L}_{\phi B}^{(2)}$ are shown in Fig. 1. The expressions for these one-loop πN amplitudes are rather tedious and will therefore not be reproduced here. The explicit analytical expressions for the loop contributions of order $\mathcal{O}(p^4)$ to elastic πN scattering can be obtained from the authors upon request. For orientation of the readers, we remark that these πN loop amplitudes are composed of the following basic loop functions:

$$J_0(w, m) = \frac{1}{i} \int \frac{d^D l}{(2\pi)^D} \frac{1}{(v \cdot l - w)(m^2 - l^2)} = \frac{w}{8\pi^2}\left(1 - 2\ln\frac{m}{\lambda}\right)$$

$$+ \begin{cases} \frac{1}{4\pi^2}\sqrt{w^2 - m^2}\ln\frac{-w+\sqrt{w^2-m^2}}{m} & (w < -m), \\ -\frac{1}{4\pi^2}\sqrt{m^2 - w^2}\arccos\frac{-w}{m} & (-m < w < m), \\ \frac{1}{4\pi^2}\sqrt{w^2 - m^2}\left(i\pi - \ln\frac{w+\sqrt{w^2-m^2}}{m}\right) & (w > m), \end{cases} \tag{8}$$

$$\frac{1}{i}\int \frac{d^D l}{(2\pi)^D} \frac{\{1, l^\mu, l^\mu l^\nu\}}{(m^2 - l^2)[m^2 - (l-k)^2]} = \left\{I_0(t,m), \frac{k^\mu}{2}I_0(t,m), g^{\mu\nu}I_2(t,m) + k^\mu k^\nu I_3(t,m)\right\}, \tag{9}$$

$$I_0(t,m) = \frac{1}{8\pi^2}\left\{\frac{1}{2} - \ln\frac{m}{\lambda} - \sqrt{1 - \frac{4m^2}{t}}\ln\frac{\sqrt{4m^2 - t} + \sqrt{-t}}{2m}\right\}, \tag{10}$$

$$I_2(t,m) = \frac{1}{48\pi^2}\left\{2m^2 - \frac{5t}{12} + \left(\frac{t}{2} - 3m^2\right)\ln\frac{m}{\lambda} - \frac{(4m^2 - t)^{3/2}}{2\sqrt{-t}}\ln\frac{\sqrt{4m^2 - t} + \sqrt{-t}}{2m}\right\}, \tag{11}$$

$$I_3(t,m) = \frac{1}{24\pi^2}\left\{\frac{7}{12} - \frac{m^2}{t} - \ln\frac{m}{\lambda} - \left(1 - \frac{m^2}{t}\right)\sqrt{1 - \frac{4m^2}{t}}\ln\frac{\sqrt{4m^2 - t} + \sqrt{-t}}{2m}\right\}. \tag{12}$$
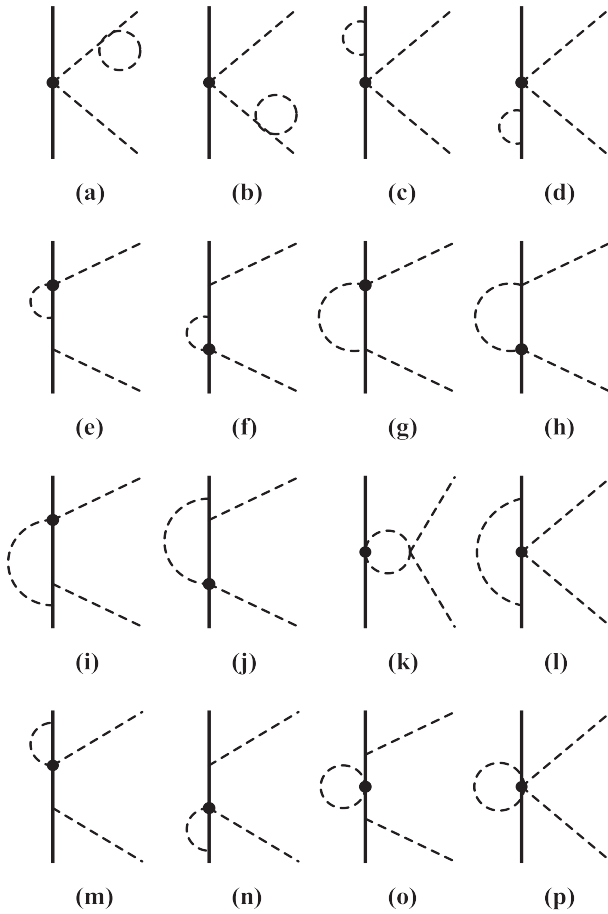

FIG. 1. Nonvanishing one-loop diagrams contributing at chiral order four. The heavy dots refer to vertices from $\mathcal{L}_{\phi B}^{(2)}$. Crossed graphs are not shown.

Note that terms proportional to the divergent constant $\lambda^{D-4}[\frac{1}{D-4} + \frac{1}{2}(\gamma_E - 1 - \ln 4\pi)]$ have been dropped. Furthermore, one observes that the one-loop amplitudes of order $\mathcal{O}(p^4)$ involve the full set of dimension-two LECs $b_i (i = D, F, 0, \ldots, 11)$ and not just the few combinations of LECs C_i $(i = 0, 1, 2, 3)$ arising from tree diagrams.

IV. PARTIAL-WAVE PHASE SHIFTS AND SCATTERING LENGTHS

The partial-wave amplitudes $f_j^{(I)}(q^2)$, where $j = l \pm 1/2$ refers to the total angular momentum and l to orbital angular momentum, are obtained from the non-spin-flip and spin-flip amplitudes by the following projection formula:

$$f_{l\pm 1/2}^{(I)}(q^2) = \frac{M_N}{8\pi\sqrt{s}}\int_{-1}^{+1} dz\{V_{\pi N}^{(I)}(w, t)P_l(z)$$
$$+ q^2 W_{\pi N}^{(I)}(w, t)[P_{l\pm 1}(z) - zP_l(z)]\}, \tag{13}$$

where $P_l(z)$ denotes the conventional Legendre polynomial, and $\sqrt{s} = \sqrt{m_\pi^2 + q^2} + \sqrt{M_N^2 + q^2}$ is the total center-of-mass energy. For the energy range considered in this paper, the phase shifts $\delta_{l\pm 1/2}^{(I)}$ are calculated as (see also Refs. [20,35])

$$\delta_{l\pm 1/2}^{(I)}(q^2) = \arctan[|q|\mathrm{Re}f_{l\pm 1/2}^{(I)}(q^2)]. \tag{14}$$

The scattering lengths for S waves and the scattering volumes for P waves are obtained by dividing out the

threshold behavior of the respective partial-wave amplitude and approaching the threshold [36]

$$a_{l\pm1/2}^{(I)} = \lim_{|\boldsymbol{q}|\to0} |\boldsymbol{q}|^{-2l} f_{l\pm1/2}^{(I)}(\boldsymbol{q}^2).$$ (15)

V. RESULTS AND DISCUSSION

Before presenting results, we have to determine the LECs. The parameters M_0, b_D, b_F, and b_0 have been determined in our previous paper by using of the four octet-baryon masses (M_N, M_Σ, M_Ξ, M_Λ) and the pion-nucleon σ term $\sigma_{\pi N} = 59.1 \pm 3.5$ MeV [26]. In this paper, we take the same value $M_0 = 646.3$ MeV, but the parameters b_0, b_D, and b_F are obtained in the fitting. Unfortunately, the 14 dimension-two LECs cannot be regrouped up to fourth order in SU(3) HBχPT. Then, in total, there are 23 unknown constants that need to be determined. Throughout this paper, we also use $m_\pi = 139.57$ MeV, $m_K = 493.68$ MeV, $m_\eta = 547.86$ MeV, $f_\pi = 92.07$ MeV, $f_K = 110.03$ MeV, $f_\eta = 1.2f_\pi$, $M_N = 938.92 \pm 1.29$ MeV, $M_\Sigma = 1191.01 \pm 4.86$ MeV, $M_\Xi = 1318.26 \pm 6.30$ MeV, $M_\Lambda = 1115.68 \pm 5.58$ MeV, $\lambda = 4\pi f_\pi = 1.16$ GeV, $D = 0.80$, and $F = 0.47$ [37–39].

We have various fitting strategies to determine the pertinent constants, and the related discussion is given in Ref. [33]. One of them is using the octet-baryon masses ($M_{N,\Sigma,\Xi,\Lambda}$) and the phase shifts of πN scattering simultaneously. This can no longer be done up to fourth order due to the appearance of the more constants for octet-baryon masses. Thus, we determine the LECs by using the πN phase shifts from RS equations [40,41]. The explicit numerical solutions for the πN phase shifts can be found in Appendix D of Ref. [41]. Note that the RS phase shifts are different from the WI08 phase shifts [42,43] and the phase shifts errors can be obtained in the RS solution. Thus, we do not need to choose an inaccurate uncertainty for all phase shifts before the fitting procedure. The choice for the RS phase shifts is also expected to improve our fitting. The data points of the S and P waves in the range of 10–200 MeV pion lab momentum are used. The resulting LECs can be found in the N3LO of Table I. The uncertainty for the respective parameter is purely estimated (for a detailed discussion, see, e.g., Refs. [44,45]). It is not surprising that most LECs are natural size $\mathcal{O}(1)$; i.e., the absolute values of these LECs are between one and ten when one introduces the dimensionless LECs (e.g., $b_i' = 2M_0 b_i$), whereas some of LECs come out fairly large. The situation also can be found in SU(2) HBχPT [21]. In fact, the dimension three LECs H_i are not terribly large. Because we have $H_1 = 4\bar{d}_5 + 2(\bar{d}_1 + \bar{d}_2)$, $H_2 = \bar{d}_1 + \bar{d}_2$, $H_3 = 2\bar{d}_3$, $H_4 = \bar{d}_{14} - \bar{d}_{15}$, where $\bar{d}_i$ are from SU(2) HBχPT. Then, we can obtain $\{\bar{d}_1 + \bar{d}_2, \bar{d}_3, \bar{d}_5, \bar{d}_{14} - \bar{d}_{15}\} = \{10.98, -4.94, 4.61, 15.48\}$GeV^{-2}. However, the results of $\bar{d}_i$ are clearly not $\mathcal{O}(1)$, which indicates the presence of additional degree of

TABLE I. Values of the various fits. The fits N3LO, N2LO, and NLO refer to the best fit up to fourth, third, and second order, respectively. For a detailed description of these fits, see the main text. Note that the ($*$) values are calculated by b_i.

	N3LO	N2LO	NLO
b_D (GeV^{-1})	-3.44 ± 0.13		
b_F (GeV^{-1})	4.64 ± 0.18		
b_0 (GeV^{-1})	-1.03 ± 0.25		
b_1 (GeV^{-1})	1.61 ± 0.08		
b_2 (GeV^{-1})	0.10 ± 0.03		
b_3 (GeV^{-1})	-4.50 ± 0.32		
b_4 (GeV^{-1})	-1.34 ± 0.17		
b_5 (GeV^{-1})	-23.28 ± 1.56		
b_6 (GeV^{-1})	1.90 ± 0.21		
b_7 (GeV^{-1})	8.96 ± 0.99		
b_8 (GeV^{-1})	-5.62 ± 0.67		
b_9 (GeV^{-1})	1.86 ± 0.23		
b_{10} (GeV^{-1})	-0.38 ± 0.00		
b_{11} (GeV^{-1})	17.66 ± 1.56		
C_0 (GeV^{-1})	$-0.86 \pm 0.55^{(*)}$	-3.59 ± 0.06	-1.69 ± 1.49
C_1 (GeV^{-1})	$-7.31 \pm 0.65^{(*)}$	-6.60 ± 0.03	-4.30 ± 0.15
C_2 (GeV^{-1})	$-3.46 \pm 2.53^{(*)}$	3.71 ± 0.05	2.94 ± 1.45
C_3 (GeV^{-1})	$1.48 \pm 0.23^{(*)}$	1.41 ± 0.01	1.37 ± 0.07
H_1 (GeV^{-2})	40.38 ± 4.12	6.26 ± 0.35	
H_2 (GeV^{-2})	10.98 ± 1.52	4.78 ± 0.07	
H_3 (GeV^{-2})	-9.88 ± 0.82	-7.65 ± 0.31	
H_4 (GeV^{-2})	-15.48 ± 0.78	-5.76 ± 0.15	
$\bar{e}_{14}$ (GeV^{-3})	0.99 ± 0.03		
$\bar{e}_{15}$ (GeV^{-3})	-26.22 ± 3.12		
$\bar{e}_{16}$ (GeV^{-3})	22.61 ± 2.93		
$\bar{e}_{17}$ (GeV^{-3})	4.57 ± 0.52		
$\bar{e}_{18}$ (GeV^{-3})	4.57 ± 0.52		
χ^2/d.o.f.	0.24	1.24	21.83

freedom. For instance, the presence of the $\Delta(1232)$ resonance can explain the values of some LECs [7,24,46,47]. The corresponding S- and P-wave phase shifts are shown by the solid lines of Fig. 2. Obviously, we obtain an excellent description of all waves. Especially, the description of the $P11$-, $P33$-, and $P13$-wave phase shifts are improved at high energies as compared to the third-order calculation. For comparison, we present results from the best fits up to third (N2LO) and second (NLO) order in Table I. Clearly, the resulting LECs have different values in the respective order. It is not surprising that the LECs at NLO and N2LO show different values. However, the LEC values at N3LO and N2LO are also very different, even an order of magnitude in some cases, which are expected to be same. Thus, for the amplitudes up to the given order, the corresponding fit to determine their respective constants is necessary. This is similar to what was found in SU(2) HBχPT [24,25]. The feature can lead to the potential convergence problems in the chiral expansion; further analysis of the threshold and subthreshold parameters is required.
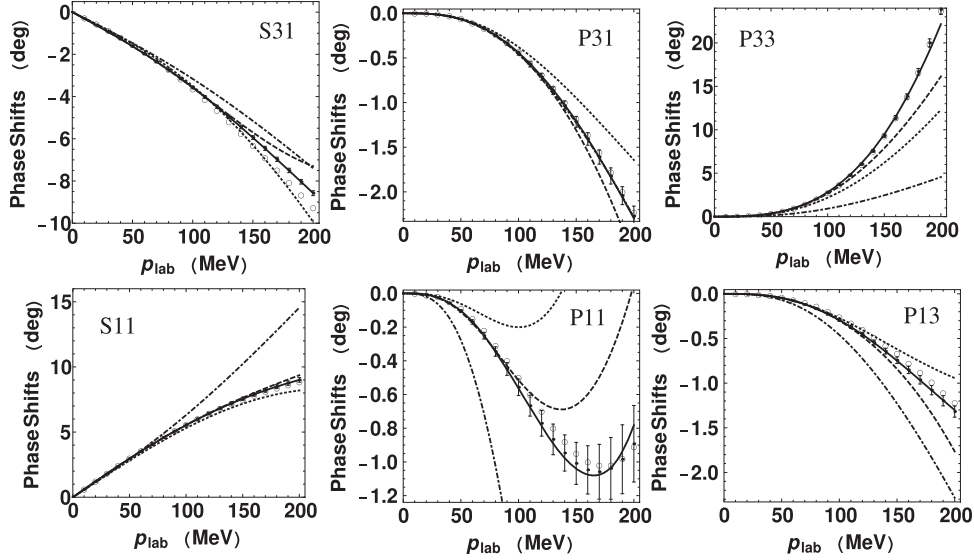
FIG. 2. Fits and predictions for pion-nucleon (πN) phase shifts from RS equations versus the pion lab momentum $|\boldsymbol{p}_{\text{lab}}|$ in πN scattering. The dot-dashed, dotted, dashed, and solid lines refer to the best fits up to first, second, third, and fourth order, respectively. The open circles denote the WI08 solution, and the data with error bars are from RS equations.

In the following, let us apply the chiral fourth-order amplitudes to estimate the threshold parameters. The analytical expressions for scattering lengths are shown in Appendix A. However, the pion-nucleon scattering lengths and scattering volumes can also be obtained by using an incident pion lab momentum $|\boldsymbol{p}_{\text{lab}}| = 5$ MeV and approximating their values at the threshold. The results are shown in Table II in comparison with the values of the various analyses. Obviously, our results for most of the threshold parameters are consistent with the ones from SU(2) HBχPT and SP98 in Ref. [21] and the RS solution in Ref. [41]. For scattering volume $a_{1+}^{1/2}$, our result is larger than the SU(2) and SP98, but it is closer to the RS solution. The values of SP98 are obtained by the use of dispersion relations with the help of a fairly precise tree-level model. In addition, there are two experimental values for scattering lengths in Table II. The values of EXP2001 are from pionic hydrogen and deuterium in Ref. [48]. The values are updated in Ref. [41] and are not shown again because they are very

close to the results from RS solution. The latter, EXPnew, are obtained by combining with the analysis of the results from Refs. [40,49–53]. As expected, our results for scattering lengths are consistent with those values within errors. In order to check the convergence, the threshold parameters from the different order are shown in Table III.

Now we discuss the subthreshold parameters. For comparing with the precise subthreshold parameters from the RS analysis [24], we consider the parameters from $D^{\pm}$ and $B^{\pm}$ amplitudes. Here, $D^{\pm} = A^{\pm} + \nu B^{\pm}$, for the detailed relations about them, see Eqs. (3.32)–(3.34) of Ref. [41]. We can obtain the subthreshold parameters from our $V^I(w, t)$ and $W^I(w, t)$ amplitudes by following Appendix E of Ref. [20]. Note that, we have $\{V, W\}^{3/2} = \{g, h\}^+ - \{g, h\}^-$ and $\{V, W\}^{1/2} = \{g, h\}^+ + 2\{g, h\}^-$ for the isospin relationship. The corresponding subthreshold parameters can be obtained by expanding our amplitudes around $(v = 0, t = 0)$. We show the results from our amplitudes with the LECs extracted from the phase shifts

TABLE II. Values of the S- and P-wave scattering lengths (fm) and scattering volumes (fm^3) in comparison with the values of the various analyses.

	Our results	SU(2)	SP98	RS	EXP2001	EXPnew
$a_{0+}^{3/2}$	$-0.122(4)$	-0.119	$-0.125(2)$	$-0.122(3)$	$-0.125(3)$	$-0.119(6)$
$a_{0+}^{1/2}$	$0.240(3)$	0.249	$0.250(2)$	$0.240(2)$	$0.250^{+0.006}_{-0.004}$	$0.235(2)$
$a_{1+}^{3/2}$	$0.603(13)$	0.586	$0.595(5)$	$0.598(8)$	$\cdots$	$\cdots$
$a_{1+}^{1/2}$	$-0.102(6)$	-0.054	$-0.038(8)$	$-0.083(3)$	$\cdots$	$\cdots$
$a_{1-}^{3/2}$	$-0.110(9)$	-0.113	$-0.122(6)$	$-0.116(3)$	$\cdots$	$\cdots$
$a_{1-}^{1/2}$	$-0.221(12)$	-0.181	$-0.207(7)$	$-0.200(11)$	$\cdots$	$\cdots$

TABLE III. Values of the S- and P-wave scattering lengths (fm) and scattering volumes (fm^3) from the different order.

	$\mathcal{O}(q)$	$\mathcal{O}(q^2)$	$\mathcal{O}(q^3)$	$\mathcal{O}(q^4)$
$a_{0+}^{3/2}$	-0.113	$-0.111(87)$	$-0.121(18)$	$-0.122(4)$
$a_{0+}^{1/2}$	0.225	$0.226(87)$	$0.240(16)$	$0.240(3)$
$a_{1+}^{3/2}$	0.241	$0.531(11)$	$0.624(15)$	$0.603(13)$
$a_{1+}^{1/2}$	-0.121	$-0.082(9)$	$-0.080(11)$	$-0.102(6)$
$a_{1-}^{3/2}$	-0.121	$-0.106(11)$	$-0.113(14)$	$-0.110(9)$
$a_{1-}^{1/2}$	-0.483	$-0.129(15)$	$-0.215(19)$	$-0.221(12)$

TABLE IV. Subthreshold parameters for the $D^{\pm}$ and $B^{\pm}$ amplitudes in comparison to the RS analysis.

	N2LO	N3LO	RS
$d_{00}^{+}[m_{\pi}^{-1}]$	$-0.91(12)$	$-0.99(15)$	$-1.36(3)$
$d_{10}^{+}[m_{\pi}^{-3}]$	$1.12(7)$	$1.21(13)$	$1.16(2)$
$d_{01}^{+}[m_{\pi}^{-3}]$	$1.30(5)$	$1.28(8)$	$1.16(2)$
$d_{20}^{+}[m_{\pi}^{-5}]$	$-0.13(6)$	$0.13(6)$	$0.196(3)$
$d_{11}^{+}[m_{\pi}^{-5}]$	$-0.011(9)$	$0.16(11)$	$0.185(3)$
$d_{02}^{+}[m_{\pi}^{-5}]$	$0.0298(18)$	$0.076(13)$	$0.0336(6)$
$b_{00}^{+}[m_{\pi}^{-3}]$	$-6.14(8)$	$-6.11(14)$	$-3.45(7)$
$d_{00}^{-}[m_{\pi}^{-2}]$	$0.93(11)$	$0.63(17)$	$1.41(1)$
$d_{10}^{-}[m_{\pi}^{-4}]$	$-0.395(21)$	$-0.12(9)$	$-0.159(4)$
$d_{01}^{-}[m_{\pi}^{-4}]$	$-0.105(13)$	$-0.24(9)$	$-0.141(5)$
$b_{00}^{-}[m_{\pi}^{-2}]$	$9.92(6)$	$9.73(8)$	$10.49(11)$
$b_{10}^{-}[m_{\pi}^{-4}]$	$0.44(5)$	$0.11(14)$	$1.00(3)$
$b_{01}^{-}[m_{\pi}^{-4}]$	$-0.28(9)$	$0.39(16)$	$0.21(2)$

up to third order (N2LO) and fourth order (N3LO) in comparison to the RS analysis in Table IV. Not surprisingly, the values from the third-order amplitudes are not precise. When using the fourth order amplitudes, we do not find an improvement of the subthreshold parameters, and in some parameters they are even clearly worse. The situation is same as in SU(2) HBχPT [20,21]. Furthermore, the

convergence problems obviously come out. Most of the subthreshold parameters from N3LO and N2LO are not consistent, and some even have opposite signs. The fact is that one cannot properly reproduce the subthreshold kinematic parameters from the amplitudes with convergence problems in the low-energy region. This is exactly similar to what is found when the scattering lengths are predicted from LECs extracted at the subthreshold point up to N2LO. Thus, we can use the subthreshold parameters to determine the LECs, as done in Ref. [24], and then discuss the pertinent physical quantity. But we have 23 LECs at fourth order in SU(3) HBχPT. That means we need 23 precise subthreshold parameters from RS analysis. This solution will be done in future works.

However, the subthreshold parameters only involve eight LECs at third order in both SU(3) and SU(2) HBχPT. That means we need the eight subthreshold parameters to determine the LECs at third order. The expressions of the subthreshold parameters in SU(3) HBχPT can be found in Appendix B. The pertinent expressions in SU(2) HBχPT can be obtained by subtracting the contributions from K and η internal meson lines in one-loop diagrams. We use the precise values of the subthreshold parameters from the RS analysis [24] to determine the same LECs in both SU(3) and SU(2) HBχPT. The results are shown in Table V. The results of SU(2) are slightly different from Ref. [24] because of the different physical quantity from Particle Data Group (PDG) was taken. Note that the errors as propagated from the subthreshold parameters are same in both SU(3) and SU(2) solutions because the expressions from K and η loop diagrams do not involve the LECs at third order. The SU(3)$_K$ presents the result that the contributions from η-meson loop diagrams is subtracted. Clearly, all LECs, except for $\bar{d}_1 + \bar{d}_2$, are obviously different in SU(2) and SU(3) solutions. Thus, it is interesting to predict the threshold parameters by using the LECs from the subthreshold parameters. Let us look at the scattering lengths as an example; for the pertinent expressions, see Appendix A. In unites of fm, we obtain

TABLE V. Results for the πN LECs at NLO and N2LO in both SU(3) and SU(2) HBχPT. The results for the c_i and $\bar{d}_i$ are given in units of GeV^{-1} and GeV^{-2}, respectively. Note that the results from SU(2) and SU(3) are the same at NLO.

	NLO							
	c_1	c_2	c_3	c_4				
SU(2)	$-0.75(4)$	$1.81(3)$	$-3.62(6)$	$2.16(3)$				
	N2LO							
	c_1	c_2	c_3	c_4	$\bar{d}_1 + \bar{d}_2$	$\bar{d}_3$	$\bar{d}_5$	$\bar{d}_{14} - \bar{d}_{15}$
SU(3)	$-1.23(4)$	$4.57(3)$	$-6.36(6)$	$4.19(3)$	$1.08(6)$	$-0.28(2)$	$0.04(4)$	$-1.56(6)$
SU(3)$_K$	$-1.23(4)$	$4.54(3)$	$-6.34(6)$	$4.16(3)$	$1.11(6)$	$-0.29(2)$	$0.04(4)$	$-1.57(6)$
SU(2)	$-1.07(4)$	$3.20(3)$	$-5.32(6)$	$3.55(3)$	$1.03(6)$	$-0.47(2)$	$0.13(4)$	$-1.89(6)$

$$a_{0+}^{3/2} = \{-0.113, -0.146, -0.130\}_{SU(2)}, \qquad \{-0.113, -0.146, -0.128\}_{SU(3)},$$
$$a_{0+}^{1/2} = \{0.225, 0.192, 0.263\}_{SU(2)}, \qquad \{0.225, 0.192, 0.266\}_{SU(3)}, \tag{16}$$

where the three entries of the arrays refer to the LO, NLO, and N2LO scattering length values, respectively. The situation $SU(3)_K$ is not shown because the contributions from η-meson loop are very small. Not surprisingly, the results from the SU(2) and SU(3) are almost the same at third order. The contributions from the kaon loops cannot improve the predictions for the scattering lengths from LECs extracted at the subthreshold point up to N2LO. Therefore, the convergence problems still exist the same as in SU(2) HBχPT [24]. The differences between the scattering lengths from Eq. (16) and Table III emphasize these convergence problems. Furthermore, we try to impose constraints to the LECs both from the threshold and subthreshold kinematic parameters to analyze whether the discrepancies improve. First, we obtain the LECs combinations $-2c_1 + c_2 + c_3 = 0.59$ GeV^{-1} and $\bar{d}_1 + \bar{d}_2 + \bar{d}_3 + 2\bar{d}_5 = 0.28$ GeV^{-2} by using the two scattering lengths from the RS solution at N2LO in SU(3) HBχPT. Then, the $c_2, c_3, \bar{d}_1 + \bar{d}_2$, and $\bar{d}_3$ are fixed by the subthreshold parameters; see Table V. Now we predict the subthreshold parameters $d_{00}^+ = -1.41[m_\pi^{-1}]$ and $d_{00}^- = 1.30[m_\pi^{-2}]$. The d_{00}^+ is very closed to the value from the RS solution, but the d_{00}^- has a certain gap. The results are disappointing. However, the inclusion of the resonance $\Delta(1232)$ might help to solve all previous observed problems.

Finally, we discuss the convergence of the chiral expansion in detail. In Fig. 2, we show the best fits up to the respective order. In all partial waves, the fourth-order corrections are smaller than the third-order ones below 150 MeV, indicating convergence. In most cases, the third-order corrections are smaller than the second-order ones. The second-order corrections are smaller than the first-order ones in a few partial waves. Therefore, the convergence of the chiral expansion becomes better along with the increase of the order. However, with the energy increasing the convergence of the chiral expansion becomes worse. It is not surprising because the chiral expansion is expanded in terms of p/Λ_χ. We can also study the convergence of the threshold parameters; see Table III. The two scattering lengths $a_{0+}^{3/2}$ and $a_{0+}^{1/2}$ from S waves are almost unchanged in a different order, indicating convergence in each order. The other four scattering volumes from P waves are consistent from order $\mathcal{O}(q^3)$. The calculation results indicate that the convergence of the threshold parameters is fast because it is due to $m_\pi/\Lambda_\chi \sim 1/7$. However, the convergence problems

obviously come out when the subthreshold parameters are considered. These problems become more complicated. A great improvement on the convergence of the chiral expansion is still necessary.

In summary, we calculated the T matrices for pion-nucleon scattering to the fourth order in SU(3) HBχPT. We fitted the RS phase shifts of πN scattering in range of 10–200 MeV pion lab momentum to determine the LECs. This led to an good description of S- and P-wave phase shifts below 200 MeV pion lab momentum. The separated LECs b_i were also obtained; they can be used as input to the other physical processes. The scattering lengths and scattering volumes were also calculated at this order, which turned out to be in agreement with those of other approaches and available experimental data. Then, we discussed the subthreshold parameters, and found that it was not a good choice to obtain the subthreshold parameters from the πN phase shifts. We also discussed the different LECs obtained by subthreshold parameters in both SU(2) and SU(3) HBχPT, and it turned out that the contribution from kaon loops can contribute to the LECs, but the prediction from subthreshold parameters to threshold parameters was not improved. Finally, the convergence of the chiral expansion was discussed in detail. To sum up, the calculation of πN scattering in SU(3) HBχPT provides the possibility to consider explicitly more complex processes involving strangeness. An improved result for πN scattering can be achieved through including the resonance $\Delta(1232)$ and the other hadronic contributions.

APPENDIX A: SCATTERING LENGTHS

In this Appendix, the analytical expressions for the scattering lengths from SU(3) HBχPT up to third order are given by

$$a_{0+}^+ = \frac{m_\pi^2[-(D+F)^2 + 8M_N(-2c_1 + c_2 + c_3) + 4m_\pi^2(D+F)\bar{d}_{18}]}{16\pi(M_N + m_\pi)f_\pi^2} + \frac{3(D+F)^2 M_N m_\pi^3}{256\pi^2(M_N + m_\pi)f_\pi^4}$$
$$- \frac{M_N m_\pi^2 \sqrt{m_K^2 - m_\pi^2}}{384\pi^3(M_N + m_\pi)f_\pi^2 f_K^2}\left(7\pi + 4\arccos\frac{m_\pi}{m_K} + 4\arcsin\frac{m_\pi}{m_K}\right) - \frac{(D-3F)^2 M_N m_\pi^2 m_\eta}{768\pi^2(M_N + m_\pi)f_\pi^2 f_\eta^2}, \tag{A1}$$

$$a_{0+}^- = \frac{M_N m_\pi}{8\pi(M_N + m_\pi)f_\pi^2} + \frac{m_\pi^3[(D+F)^2 + 32M_N^2(\bar{d}_1 + \bar{d}_2 + \bar{d}_3 + 2\bar{d}_5)]}{32\pi M_N(M_N + m_\pi)f_\pi^2} + \frac{M_N m_\pi^3}{64\pi^3(M_N + m_\pi)f_\pi^4}$$
$$- \frac{M_N m_\pi^2}{384\pi^3(M_N + m_\pi)f_\pi^2 f_K^2}\left[-3m_\pi + \sqrt{m_K^2 - m_\pi^2}\left(\pi - 2\arccos\frac{m_\pi}{m_K} + 4\arcsin\frac{m_\pi}{m_K}\right)\right], \tag{A2}$$

where we use the physical decay constants $f_\pi^2 f_K^2$ and $f_\pi^2 f_\eta^2$ in K and η internal meson lines from one-loop diagrams, respectively. Note that, for comparing with the results from SU(2) HBχPT, the same LECs ($c_i, \bar{d}_i$) are used. For the isospin relationship, we also have $a_{0+}^{3/2} = a_{0+}^+ - a_{0+}^-$ and $a_{0+}^{1/2} = a_{0+}^+ + 2a_{0+}^-$.

APPENDIX B: SUBTHRESHOLD PARAMETERS

In this Appendix we present the expressions for the subthreshold parameters from the third order amplitudes in SU(3) HBχPT. In the same conventions with the scattering lengths, the subthreshold parameters read

$$d_{00}^+ = -\frac{2(2c_1 - c_3)m_\pi^2}{f_\pi^2} + \frac{(D+F)^2[3 + 8(D+F)^2]m_\pi^3}{64\pi f_\pi^4} + \frac{1}{192\pi f_\pi^2 f_K^2}(19D^4 + 12D^3 F$$
$$+ 58D^2 F^2 - 36DF^3 + 75F^4)m_K m_\pi^2 + \frac{1}{192\pi f_\pi^2 f_\eta^2}(D - 3F)^2[-1 + 4(D+F)^2]m_\eta m_\pi^2, \tag{B1}$$

$$d_{10}^+ = \frac{2c_2}{f_\pi^2} - \frac{[4 + 5(D+F)^4]m_\pi}{32\pi f_\pi^4} - \frac{1}{768\pi f_\pi^2 f_K^2 m_K}[72m_K^2 + (19D^4 + 12D^3 F + 58D^2 F^2$$
$$- 36DF^3 + 75F^4)(m_\pi^2 + 4m_K^2)] - \frac{1}{192\pi f_\pi^2 f_\eta^2 m_\eta}(D - 3F)^2(D + F)^2(m_\pi^2 + 4m_\eta^2), \tag{B2}$$

$$d_{01}^+ = -\frac{c_3}{f_\pi^2} - \frac{(D+F)^2[77 + 48(D+F)^2]m_\pi}{768\pi f_\pi^4} - \frac{1}{384\pi f_\pi^2 f_K^2}(15D^2 - 18DF + 27F^2 + 19D^4 + 75F^4$$
$$+ 58D^2 F^2 - 36DF^3 + 12D^3 F)m_K + \frac{1}{6912\pi f_\pi^2 f_\eta^2 m_\eta}(D - 3F)^2[5m_\pi^2 - 72(D+F)m_\eta^2], \tag{B3}$$

$$d_{00}^- = \frac{1}{2f_\pi^2} + \frac{4m_\pi^2(\bar{d}_1 + \bar{d}_2 + 2\bar{d}_5)}{f_\pi^2} + \frac{(D+F)^4 m_\pi^2}{48\pi^2 f_\pi^4} + \frac{1}{288\pi^2 f_\pi^2 f_K^2}(23D^4 - 20D^3 F - 14D^2 F^2$$
$$+ 60DF^3 + 111F^4)m_\pi^2 + \frac{1}{36\pi^2 f_\pi^2 f_\eta^2}(D - 3F)^2(D + F)^2 m_\pi^2, \tag{B4}$$

$$d_{10}^- = \frac{4\bar{d}_3}{f_\pi^2} - \frac{15 + 7(D+F)^4}{240\pi^2 f_\pi^4} - \frac{1}{1440\pi^2 f_\pi^2 f_K^2 m_K^2}[5(9 + 23D^4 - 20D^3 F - 14D^2 F^2 + 60DF^3$$
$$+ 111F^4)m_K^2 + 2(17D^4 - 12D^3 F - 2D^2 F^2 + 36DF^3 + 57F^4)m_\pi^2]$$
$$- \frac{1}{180\pi^2 f_\pi^2 f_\eta^2 m_\eta^2}(D - 3F)^2(D + F)^2(m_\pi^2 + 5m_\eta^2), \tag{B5}$$

$$d_{01}^- = -\frac{2(\bar{d}_1 + \bar{d}_2)}{f_\pi^2} - \frac{1 + 7(D+F)^2 + 2(D+F)^4}{192\pi^2 f_\pi^4} + \frac{1}{3456\pi^2 f_\pi^2 f_K^2}[39 - 47D^2 + 282DF + 141F^2$$
$$- 138D^4 + 120D^3 F + 84D^2 F^2 - 360DF^3 - 666F^4] - \frac{1}{72\pi^2 f_\pi^2 f_\eta^2}(D - 3F)^2(D + F)^2, \tag{B6}$$

$$b_{00}^{+} = \frac{4M_N(\bar{d}_{14} - \bar{d}_{15})}{f_\pi^2} - \frac{(D+F)^4 M_N}{8\pi^2 f_\pi^4} - \frac{1}{432\pi^2 f_\pi^2 f_K^2}(47D^4 + 60D^3F + 18D^2F^2 + 108DF^3$$

$$+ 279F^4)M_N - \frac{1}{24\pi^2 f_\pi^2 f_\eta^2}(D-3F)^2(D+F)^2 M_N, \tag{B7}$$

$$b_{00}^{-} = \frac{1}{2f_\pi^2} + \frac{2c_4 M_N}{f_\pi^2} - \frac{(D+F)^2[1+(D+F)^2]M_N m_\pi}{8\pi f_\pi^4} - \frac{1}{96\pi f_\pi^2 f_K^2}(2D^2 - 12DF - 6F^2 + 9D^4$$

$$+ 20D^3F - 2D^2F^2 + 36DF^3 + 33F^4)M_N m_K - \frac{1}{48\pi f_\pi^2 f_\eta^2}(D-3F)^2(D+F)^2 M_N m_\eta. \tag{B8}$$

[1] S. Weinberg, Phenomenological Lagrangians, Physica (Amsterdam) **96A**, 327 (1979).

[2] J. Gasser and H. Leutwyler, Chiral perturbation theory to one loop, Ann. Phys. (N.Y.) **158**, 142 (1984).

[3] H. Leutwyler, On the foundations of chiral perturbation theory, Ann. Phys. (N.Y.) **235**, 165 (1994).

[4] S. Scherer and M. R. Schindler, A primer for chiral perturbation theory, Lect. Notes Phys. **830**, 1 (2012).

[5] E. E. Jenkins and A. V. Manohar, Baryon chiral perturbation theory using a heavy fermion Lagrangian, Phys. Lett. B **255**, 558 (1991).

[6] V. Bernard, N. Kaiser, J. Kambor, and U.-G. Meißner, Chiral structure of the nucleon, Nucl. Phys. **B388**, 315 (1992).

[7] T. Becher and H. Leutwyler, Baryon chiral perturbation theory in manifestly Lorentz invariant form, Eur. Phys. J. C **9**, 643 (1999).

[8] J. Gegelia and G. Japaridze, Matching heavy particle approach to relativistic theory, Phys. Rev. D **60**, 114038 (1999).

[9] T. Fuchs, J. Gegelia, G. Japaridze, and S. Scherer, Renormalization of relativistic baryon chiral perturbation theory and power counting, Phys. Rev. D **68**, 056005 (2003).

[10] M. R. Schindler, T. Fuchs, J. Gegelia, and S. Scherer, Axial, induced pseudoscalar, and pion-nucleon form-factors in manifestly Lorentz-invariant chiral perturbation theory, Phys. Rev. C **75**, 025202 (2007).

[11] L. S. Geng, J. Martin Camalich, L. Alvarez-Ruso, and M. J. Vicente Vacas, Leading SU(3)-Breaking Corrections to the Baryon Magnetic Moments in Chiral Perturbation Theory, Phys. Rev. Lett. **101**, 222002 (2008).

[12] J. Martin Camalich, L. S. Geng, and M. J. Vicente Vacas, The lowest-lying baryon masses in covariant SU(3)-flavor chiral perturbation theory, Phys. Rev. D **82**, 074504 (2010).

[13] X. L. Ren, L. S. Geng, J. Martin Camalich, J. Meng, and H. Toki, Octet baryon masses in next-to-next-to-next-to-leading order covariant baryon chiral perturbation theory, J. High Energy Phys. 12 (2012) 073.

[14] J. M. Alarcón, J. Martin Camalich, and J. A. Oller, The chiral representation of the πN scattering amplitude and the pion-nucleon sigma term, Phys. Rev. D **85**, 051503 (2012).

[15] J. M. Alarcón, J. Martin Camalich, and J. A. Oller, Improved description of the πN scattering phenomenology in covariant baryon chiral perturbation theory, Ann. Phys. (Amsterdam) **336**, 413 (2013); J. M. Alarcón (private communication).

[16] L.-S. Geng, Recent developments in SU(3) covariant baryon chiral perturbation theory, Front. Phys. **8**, 328 (2013).

[17] Y.-H. Chen, D.-L. Yao, and H. Q. Zheng, Analyses of pion-nucleon elastic scattering amplitudes up to $\mathcal{O}(p^4)$ in extended-on-mass-shell subtraction scheme, Phys. Rev. D **87**, 054019 (2013).

[18] D.-L. Yao, D. Siemens, V. Bernard, E. Epelbaum, A. M. Gasparyan, J. Gegelia, H. Krebs, and U.-G. Meißner, Pion-nucleon scattering in covariant baryon chiral perturbation theory with explicit Delta resonances, J. High Energy Phys. 05 (2016) 038.

[19] J.-X. Lu, L.-S. Geng, X.-L. Ren, and M.-L. Du, Meson-baryon scattering up to the next-to-next-to-leading order in covariant baryon chiral perturbation theory, Phys. Rev. D **99**, 054024 (2019).

[20] N. Fettes, U.-G. Meißner, and S. Steininger, Pion-nucleon scattering in chiral perturbation theory (I): Isospin symmetric case, Nucl. Phys. **A640**, 199 (1998).

[21] N. Fettes and U.-G. Meißner, Pion nucleon scattering in chiral perturbation theory (II): Fourth order calculation, Nucl. Phys. **A676**, 311 (2000).

[22] H. Krebs, A. Gasparyan, and E. Epelbaum, Chiral three-nucleon force at N4LO I: Longest-range contributions, Phys. Rev. C **85**, 054006 (2012).

[23] D. R. Entem, N. Kaiser, R. Machleidt, and Y. Nosyk, Peripheral nucleon-nucleon scattering at fifth order of chiral perturbation theory, Phys. Rev. C **91**, 014002 (2015).

[24] M. Hoferichter, J. Ruiz de Elvira, B. Kubis, and U.-G. Meißner, Matching Pion-Nucleon Roy-Steiner Equations to Chiral Perturbation Theory, Phys. Rev. Lett. **115**, 192301 (2015).

[25] D. Siemens, J. Ruiz de Elvira, E. Epelbaum, M. Hoferichter, H. Krebs, B. Kubis, and U.-G. Meißner, Reconciling threshold and subthreshold expansions for pion-nucleon scattering, Phys. Lett. B **770**, 27 (2017).

[26] B.-L. Huang and Y.-D. Li, Kaon-nucleon scattering to one-loop order in heavy baryon chiral perturbation theory, Phys. Rev. D **92,** 114033 (2015); Erratum, Phys. Rev. D **95,** 019903 (2017).

[27] B.-L. Huang, J.-S. Zhang, Y.-D. Li, and N. Kaiser, Meson-baryon scattering to one-loop order in heavy baryon chiral perturbation theory, Phys. Rev. D **96,** 016021 (2017).

[28] N. Kaiser, Chiral corrections to kaon nucleon scattering lengths, Phys. Rev. C **64,** 045204 (2001); Erratum, Phys. Rev. C **73,** 069902 (2006).

[29] Y.-R. Liu and S.-L. Zhu, Meson-baryon scattering lengths in HBχPT, Phys. Rev. D **75,** 034003 (2007).

[30] Y.-R. Liu and S.-L. Zhu, Decuplet contribution to the meson-baryon scattering lengths, Eur. Phys. J. C **52,** 177 (2007).

[31] Z.-W. Liu, Y.-R. Liu, and S.-L. Zhu, Pseudoscalar meson and decuplet baryon scattering lengths, Phys. Rev. D **83,** 034004 (2011).

[32] Z.-W. Liu and S.-L. Zhu, Pseudoscalar meson and charmed baryon scattering lengths, Phys. Rev. D **86,** 034009 (2012); Erratum, Phys. Rev. D **93,** 019901 (2016).

[33] B.-L. Huang and J. Ou-Yang, Pion-nucleon scattering to $\mathcal{O}(p^3)$ in heavy baryon SU(3) chiral perturbation theory, Phys. Rev. D **101,** 056021 (2020).

[34] S.-Z. Jiang, Q.-S. Chen, and Y.-R. Liu, Meson-baryon effective chiral Lagrangians at order p^4, Phys. Rev. D **95,** 014012 (2017).

[35] J. Gasser and U.-G. Meißner, On the phase of epsilon-prime, Phys. Lett. B **258,** 219 (1991).

[36] T. E. O. Ericson and W. Weise, *Pions and Nuclei* (Clarendon Press, Oxford, UK, 1988).

[37] M. Tanabashi *et al.*, Review of Particle Physics, Phys. Rev. D **98,** 030001 (2018).

[38] C. C. Chang *et al.*, A per-cent-level determination of the nucleon axial coupling from quantum chromodynamics, Nature (London) **558,** 91 (2018).

[39] B. Märkisch *et al.*, Measurement of the Weak Axial-Vector Coupling Constant in the Decay of Free Neutrons Using a Pulsed Cold Neutron Beam, Phys. Rev. Lett. **122,** 242501 (2019).

[40] M. Hoferichter, J. Ruiz de Elvira, B. Kubis, and U.-G. Meißner, High-Precision Determination of the Pion-Nucleon σ-Term from Roy-Steiner Equations, Phys. Rev. Lett. **115,** 092301 (2015).

[41] M. Hoferichter, J. Ruiz de Elvira, B. Kubis, and U.-G. Meißner, Roy-Steiner-equation analysis of pion-nucleon scattering, Phys. Rep. **625,** 1 (2016).

[42] W. J. Briscoe *et al.*, SAID on-line program, see http://gwdac.phys.gwu.edu.

[43] R. L. Workman, R. A. Arndt, W. J. Briscoe, M. W. Paris, and I. I. Strakovsky, Parameterization dependence of T matrix poles and eigenphases from a fit to πN elastic scattering data, Phys. Rev. C **86,** 035202 (2012).

[44] J. Dobaczewski, W. Nazarewicz, and P.-G. Reinhard, Error estimates of theoretical models: A guide, J. Phys. G **41,** 074001 (2014).

[45] B. D. Carlsson, A. Ekström, C. Forssén, D. Fahlin Strömberg, G. R. Jansen, O. Lilja, M. Lindby, B. A. Mattsson, and K. A. Wendt, Uncertainty Analysis and Order-By-Order Optimization of Chiral Nuclear Interactions, Phys. Rev. X **6,** 011019 (2016).

[46] V. Bernard, N. Kaiser, and U.-G. Meißner, Chiral dynamics in nucleons and nuclei, Int. J. Mod. Phys. E **04,** 193 (1995).

[47] V. Bernard, N. Kaiser, and U.-G. Meissner, Aspects of chiral pion-nucleon physics, Nucl. Phys. **A615,** 483 (1997).

[48] H. C. Schroder *et al.*, The pion nucleon scattering lengths from pionic hydrogen and deuterium, Eur. Phys. J. C **21,** 473 (2001).

[49] V. Baru, C. Hanhart, M. Hoferichter, B. Kubis, A. Nogga, and D. R. Phillips, Precision calculation of the $\pi^- d$ scattering length and its impact on threshold πN scattering, Phys. Lett. B **694,** 473 (2011).

[50] V. Baru, C. Hanhart, M. Hoferichter, B. Kubis, A. Nogga, and D. R. Phillips, Precision calculation of threshold $\pi^- d$ scattering, πN scattering lengths, and the GMO sum rule, Nucl. Phys. **A872,** 69 (2011).

[51] M. Hoferichter, V. Baru, C. Hanhart, B. Kubis, A. Nogga, and D. R. Phillips, Isospin breaking in pion deuteron scattering and the pion nucleon scattering lengths, Proc. Sci., CD12 (**2013**) 093.

[52] M. Hennebach *et al.*, Hadronic shift in pionic hydrogen, Eur. Phys. J. A **50,** 190 (2014); Erratum, Eur. Phys. J. A **55,** 24 (2019).

[53] J. Ruiz de Elvira, M. Hoferichter, B. Kubis, and U.-G. Meißner, Extracting the σ-term from low-energy pion-nucleon scattering, J. Phys. G **45,** 024001 (2018).